Order-parameter flow in the SK spin glass. I. Replica symmetry

1994 J. Phys. A: Math. Gen. 27 7687

(http://iopscience.iop.org/0305-4470/27/23/013)

J. Phys. A: Math. Gen. 27 (1994) 7687–7707. Printed in the UK

Order-parameter flow in the SK spin glass I: replica symmetry

A C C Coolen and D Sherrington

Department of Physics—Theoretical Physics, University of Oxford, 1 Keble Road, Oxford OX1 3NP, UK

Received 28 June 1994

Abstract. We present a theory to describe the dynamics of the Sherrington–Kirkpatrick spin-glass with (sequential) Glauber dynamics in terms of deterministic flow equations for macroscopic parameters. Two transparent assumptions allow us to close the macroscopic laws. Replica theory enters as a tool in the calculation of the time-dependent local field distribution. The theory produces, in a natural way, dynamical generalizations of the AT- and zero-entropy lines and of Parisi's order-parameter function $P(q)$. In equilibrium we recover the standard results from equilibrium statistical mechanics. In this paper we make the replica-symmetric ansatz, as a first step towards calculating the order-parameter flow. Numerical simulations support our assumptions and suggest that our equations describe the shape of the local field distribution and the macroscopic dynamics reasonably well in the region where replica symmetry is stable.

1. Introduction

The Sherrington–Kirkpatrick (SK) spin-glass model [1] describes a collection of N Ising spins, coupled by exchange interactions which are drawn at random from a Gaussian distribution. These interactions represent quenched (frozen) disorder. The equilibrium statistical-mechanical description of the SK model seems to have reached a stable fixed-point, built on replica theory with, at least in the spin-glass phase, broken replica symmetry *à la* Parisi [2]. A clear and extensive description of the formalism developed since 1975 and most of the relevant references can be found in textbooks like the ones by Mezard *et al* [3] and Fisher and Hertz [4].

With respect to the dynamical properties of the SK model, the situation seems different. The early dynamical studies, like [5–7], were more or less of a pilot character, employing mean-field approximations (MFA) and linearizations of the exact dynamic ensemble averages. Analytical work beyond MFA published so far has mostly concentrated on Langevin dynamics for soft spins, as opposed to Ising spins [8–11]. In the Langevin case the standard procedure (described in detail in, for example, [12, 4]) is to construct a generating functional from a path-integral representation of the microscopic state probability, which can subsequently be averaged over the quenched disorder (i.e. the random exchange interactions). This leads to a saddle-point problem, the limit $N \to \infty$ can be taken and one obtains a complicated set of equations for correlation and response functions. These can be interpreted in terms of a Langevin equation for a single spin with a retarded self-interaction and a noise term with non-trivial moments. In order to proceed from this stage, additional assumptions, restrictions or approximations are needed, like expansions near critical lines or near equilibrium. By

0305-4470/94/237687+21$19.50

construction, in these theories only time-scales which do not diverge with N are described. The approach followed by Sompolinsky in [8] is different: here a hierarchy of time-scales is introduced, all of which diverge for $N \to \infty$, but in a strict order. The case of Glauber [13] dynamics for Ising spins was studied by Sommers [14], who developed a path-integral formalism by performing manipulations on the solution (in the form of a time-ordered product) of the master equation. His method, although subsequently applied by other authors to related models like the non-symmetric SK model [15], was later criticized by Lusakowski [16]. As far as we are aware, the issue of the correctness (or otherwise) of the Sommers approach has not been settled.

At zero temperature the SK model shows strong remanence effects (see, for example, Kinzel [17]), with a non-exponential decay of the magnetization. Only recently has numerical evidence been published [18] which suggests that infinite-range models such as the SK model even exhibit ageing effects of the type observed in experiments on real spin-glasses [4, 19], which until now were always assumed to be typical for finite-range models and therefore explained using scaling arguments for growing domains.

Motivated by the non-trivial dynamical phenomena exhibited by the SK model and by the restricted theoretical understanding of the Glauber dynamics (as opposed to the continuous Langevin approach), in this paper we develop a theory to describe the Glauber dynamics of the SK model in terms of deterministic flow equations for two macroscopic state variables: the magnetization m and the spin-glass contribution r to the energy. Our reasons for choosing these two quantities as dynamic-order parameters, in favour of a dynamical equivalent of the spin-glass order parameter q or its distribution $P(q)$, are the following.

(i) On finite time-scales both m and r evolve deterministically in time in the limit $N \to \infty$.
(ii) The Hamiltonian of the SK model can be expressed solely in terms of m and r.
(iii) In thermal equilibrium m and r are self-averaging with respect to the quenched disorder in the limit $N \to \infty$ (since m and the free energy are [20]).
(iv) Both m and r are instantaneous functions of time for a single system, whereas $P(q)$ involves correlations between different times or systems.

The key to closing the deterministic laws is to calculate the distribution of time-dependent local alignment fields. Two transparent physical assumptions allow us to calculate this distribution analytically and find a *closed* set of flow equations for our two order parameters. The theory produces in a natural way dynamical generalizations of the AT- and zero-entropy lines and of Parisi's order-parameter function $P(q)$. In equilibrium we recover the standard results from equilibrium statistical mechanics. The present formalism has previously been applied successfully to a related model: the Hopfield neural network model near saturation [21].

In our view, the main appeal of our formalism is its transparency. The theory is formulated in terms of two directly observable macroscopic state variables and, apart from two simple assumptions, is derived directly from the microscopic stochastic equations. Secondly, an interesting difference with existing approaches is the way in which replica theory enters. In the standard Langevin approach (after having taken the limit $N \to \infty$) one ends up with quantities and equations very much like the ones encountered in equilibrium replica theory, with replica indices replaced by time arguments. In Sompolinsky's theory replica indices are replaced by labels of the hierarchy of time-scales. In contrast, in the present formalism replica theory enters as a mathematical tool in calculating the time-dependent distribution of local alignment fields. The only uncertainty in the status of the theory originates from the two closure assumptions, since all subsequent calculations can, in principle, be performed exactly. Both are supported to a certain extent by evidence from

numerical simulations. A recent study of an exactly solvable toy model [22], stimulated by the work reported here and in [21], suggests that the proposed closure procedure succeeds in capturing the main physics in a closed set of transparent deterministic equations and is exact for $t = 0$ and $t = \infty$, but does not reproduce all temporal characteristics for intermediate times. Since the closure procedure is based on the elimination of microscopic memory effects, the theory can contribute to a better understanding of the relation between the microscopic processes and correlations and the macroscopic measures of complexity, such as the order parameter $P(q)$.

In this paper we develop the general formalism. However, in calculating the order-parameter flow explicitly we will make the replica-symmetric RS ansatz. We will show that in most of the flow diagram replica symmetry is stable. In the region where the RS solution is unstable the flow *direction* is still described correctly and the RS theory even predicts non-exponential relaxation for $T \to 0$, but the RS equations fail to describe a rigorous slowing down which, according to simulations, sets in near the de Almeida–Thouless [23] line. In a subsequent paper we shall address the implications of replica-symmetry breaking.

2. Dynamics of the Sherrington–Kirkpatrick spin-glass

2.1. Definitions and macroscopic laws

The Sherrington–Kirkpatrick (SK) spin-glass model [1] describes N Ising spins $\sigma_i \in \{-1, 1\}$ with infinite-range exchange interactions J_{ij}:

$$J_{ij} = \frac{1}{N} J_0 + \frac{1}{\sqrt{N}} J z_{ij} \qquad i < j \tag{1}$$

where the quantities z_{ij}, which represent quenched disorder, are drawn *independently* at random from a Gaussian distribution with $\langle z_{ij} \rangle = 0$ and $\langle z_{ij}^2 \rangle = 1$.

The evolution in time of the microscopic state probability $p_t(\boldsymbol{\sigma})$ is of the Glauber [13] form, described by a continuous-time master equation,

$$\frac{\mathrm{d}}{\mathrm{d}t} p_t(\boldsymbol{\sigma}) = \sum_{k=1}^{N} [p_t(F_k\boldsymbol{\sigma}) w_k(F_k\boldsymbol{\sigma}) - p_t(\boldsymbol{\sigma}) w_k(\boldsymbol{\sigma})] \tag{2}$$

in which F_k is a spin-flip operator $F_k \Phi(\boldsymbol{\sigma}) \equiv \Phi(\sigma_1, \ldots, -\sigma_k, \ldots, \sigma_N)$ and the transition rates $w_k(\boldsymbol{\sigma})$ are

$$w_k(\boldsymbol{\sigma}) \equiv \tfrac{1}{2}[1 - \sigma_k \tanh[\beta h_k(\boldsymbol{\sigma})]] \qquad h_i(\boldsymbol{\sigma}) \equiv \sum_{j \neq i} J_{ij}\sigma_j + \theta$$

which leads to the required standard equilibrium distribution

$$p_{\mathrm{eq}}(\boldsymbol{\sigma}) \sim \mathrm{e}^{-\beta H(\boldsymbol{\sigma})} \qquad H(\boldsymbol{\sigma}) \equiv -\sum_{i<j} \sigma_i J_{ij} \sigma_j - \sum_i \theta_i \sigma_i$$

(for numerical simulations we resort to a discrete-time sequential process, where the $w_k(\boldsymbol{\sigma})$ are interpreted as transition probabilities with iteration steps of duration $1/N$. For $N \to \infty$ this must reproduce the physics of the continuous-time equation [24]). The energy per spin can be written in terms of two macroscopic quantities

$$m(\boldsymbol{\sigma}) = \frac{1}{N} \sum_i \sigma_i \qquad r(\boldsymbol{\sigma}) = \frac{1}{N\sqrt{N}} \sum_{i<j} \sigma_i z_{ij} \sigma_j \tag{3}$$

$$H(\boldsymbol{\sigma})/N = -\tfrac{1}{2} J_0 m^2(\boldsymbol{\sigma}) - \theta m(\boldsymbol{\sigma}) - J r(\boldsymbol{\sigma}) + \tfrac{1}{2} J_0/N\,. \tag{4}$$

These two observables, the magnetization and the energy contribution induced by the quenched variables $\{z_{ij}\}$, will be used to define a *macroscopic state*. The corresponding macroscopic probability distribution is

$$\mathcal{P}_t(m,r) \equiv \sum_{\sigma} p_t(\sigma)\,\delta[m-m(\sigma)]\,\delta[r-r(\sigma)]\,. \tag{5}$$

By inserting the microscopic equation (2) and after defining the 'discrete derivatives' $\Delta_i f(\sigma) \equiv f(F_i\sigma) - f(\sigma)$, we obtain

$$\begin{aligned}\frac{\mathrm{d}}{\mathrm{d}t}\mathcal{P}_t(m,r) = &-\frac{\partial}{\partial m}\left\{P_t(m,r)\left\langle\sum_{i=1}^{N} w_i(\sigma)\Delta_i m(\sigma)\right\rangle_{m,r;t}\right\}\\ &-\frac{\partial}{\partial r}\left\{P_t(m,r)\left\langle\sum_{i=1}^{N} w_i(\sigma)\Delta_i r(\sigma)\right\rangle_{m,r;t}\right\} + \mathcal{O}(N\Delta^2)\end{aligned} \tag{6}$$

with the sub-shell average

$$\langle\Phi(\sigma)\rangle_{m,r;t} \equiv \frac{\sum_{\sigma} p_t(\sigma)\delta[m-m(\sigma)]\,\delta[r-r(\sigma)]\,\Phi(\sigma)}{\sum_{\sigma} p_t(\sigma)\delta[m-m(\sigma)]\,\delta[r-r(\sigma)]}\,.$$

The local alignment fields and the 'discrete derivatives' are given by

$$h_i(\sigma) = J_0 m(\sigma) + J z_i(\sigma) + \theta + \mathcal{O}\left(\frac{1}{N}\right) \qquad z_i(\sigma) \equiv \frac{1}{\sqrt{N}}\sum_{j\neq i} z_{ij}\sigma_j$$

$$\Delta_i m(\sigma) = -\frac{2}{N}\sigma_i \qquad \Delta_i r(\sigma) = -\frac{2}{N}\sigma_i z_i(\sigma)\,.$$

With these expressions and the transition rates (2) we can evaluate (6):

$$\begin{aligned}\frac{\mathrm{d}}{\mathrm{d}t}\mathcal{P}_t(m,r) = &-\frac{\partial}{\partial m}\left\{P_t(m,r)\left[\left\langle\frac{1}{N}\sum_{i=1}^{N}\tanh\beta\,(J_0 m + J z_i(\sigma) + \theta)\right\rangle_{m,r;t} - m\right]\right\}\\ &-\frac{\partial}{\partial r}\left\{P_t(m,r)\left[\left\langle\frac{1}{N}\sum_{i=1}^{N} z_i(\sigma)\tanh\beta\,(J_0 m + J z_i(\sigma) + \theta)\right\rangle_{m,r;t} - 2r\right]\right\}\\ &+\mathcal{O}\left(\frac{1}{N}\right).\end{aligned} \tag{7}$$

In the limit $N\to\infty$ (7) acquires the Liouville form and describes deterministic flow at the macroscopic level (m,r). The evolution of the dynamic-order parameters (m,r) is governed by the flow equations

$$\frac{\mathrm{d}}{\mathrm{d}t}m = \int \mathrm{d}z\, D_{m,r;t}[z]\tanh\beta\,(J_0 m + Jz + \theta) - m \tag{8}$$

$$\frac{\mathrm{d}}{\mathrm{d}t}r = \int \mathrm{d}z\, D_{m,r;t}[z]\, z\tanh\beta\,(J_0 m + Jz + \theta) - 2r\,. \tag{9}$$

All complicated terms are concentrated in the distribution of spin-glass contributions $z_i(\sigma)$ to the local fields

$$D_{m,r;t}[z] \equiv \lim_{N\to\infty}\frac{\sum_{\sigma} p_t(\sigma)\delta[m-m(\sigma)]\,\delta[r-r(\sigma)]\,(1/N)\sum_i \delta[z-z_i(\sigma)]}{\sum_{\sigma} p_t(\sigma)\delta[m-m(\sigma)]\,\delta[r-r(\sigma)]}\,. \tag{10}$$

Thus far no approximations have been used; equations (8) and (9) are exact for $N\to\infty$.

2.2. *Closure of the macroscopic laws*

The flow equations are not yet closed: they contain the distribution $D_{m,r;t}[z]$ (10), which is defined in terms of the solution $p_t(\sigma)$ of the microscopic equation (2). In order to close the set (8) and (9) we make two simple assumptions on the asymptotic ($N \to \infty$) form of the local field distribution $D_{m,r;t}[z]$.

(i) The deterministic laws describing the evolution in time of the order parameters (m, r) are *self-averaging* with respect to the distribution of the quenched contributions z_{ij} to the exchange interactions. Therefore the local field distribution $D_{m,r;t}[z]$ is self-averaging as well.

(ii) In view of (i) we assume that, as far as the calculation of $D_{m,r;t}[z]$ is concerned, we may assume equipartitioning of probability in the macroscopic (m, r) subshells of the ensemble.

Assumption (i) allows us to simplify the problem by performing an average over the (quenched) random variables $\{z_{ij}\}$. As a consequence of assumption (ii) the explicit time-dependence in the flow equations (8) and (9), and the dependence on microscopic initial conditions are removed, since the distribution $D_{m,r;t}[z]$ will be replaced by

$$D_{m,r}[z] \equiv \lim_{N\to\infty} \left\langle \frac{\sum_\sigma \delta[m - m(\sigma)]\,\delta[r - r(\sigma)]\,(1/N)\sum_i \delta[z - z_i(\sigma)]}{\sum_\sigma \delta[m - m(\sigma)]\,\delta[r - r(\sigma)]} \right\rangle_{\{z_{ij}\}} . \tag{11}$$

For sequential dynamics, the first of our two assumptions is clearly supported by experimental evidence (sequential simulations at $T = 0.1$), which we present in figure 1 (for $J_0 = 0$, where the system evolves towards a true spin-glass state), figure 2 (for $J_0 = 1$, which marks the onset of a non-zero equilibrium magnetization) and figure 3 (for $J_0 = 2$, where the system evolves towards a ferromagnetic state). Each of the flow graphs corresponds to one particular realization of the quenched disorder $\{z_{ij}\}$. The initial states generating the different trajectories (labelled by $\ell = 0, \ldots, 10$) were drawn at random according to $p_0(\sigma) \equiv \prod_i \left[\frac{1}{2}\left[1+\frac{1}{10}\ell\right]\delta_{\sigma_i,1} + \frac{1}{2}\left[1-\frac{1}{10}\ell\right]\delta_{s_i,-1}\right]$, such that that $\langle m\rangle_{t=0} = 0.1\ell$ and $\langle r\rangle_{t=0} = 0$. With increasing system size, fluctuations in individual trajectories eventually vanish and well defined flow lines emerge, which no longer depend on the disorder realization. The second closure assumption can only be tested in such a direct manner by comparing the actual local field distribution, measured during simulations, with the result of evaluating (11). This will be done in a subsequent section.

In equilibrium studies the above two assumptions are, in fact, the basic building blocks of analysis as well, where (i) is assumed and (ii) is a consequence of the Boltzmann form of the microscopic equilibrium distribution. Our aim is to calculate analytically the $N \to \infty$ flow illustrated in figures 1–3, by combining (8) and (9) with (11). The distribution (11) will be calculated using the replica method.

2.3. *The local field distribution*

We use the following replica expression for writing expectation values of a given state variable Φ over a given measure W:

$$\langle \Phi(\sigma)\rangle_W \equiv \frac{\langle \Phi(\sigma)W(\sigma)\rangle_\sigma}{\langle W(\sigma)\rangle_\sigma} = \lim_{n\to 0} \langle \Phi(\sigma^1)\prod_{\alpha=1}^{n} W(\sigma^\alpha)\rangle_{\{\sigma^\alpha\}}$$

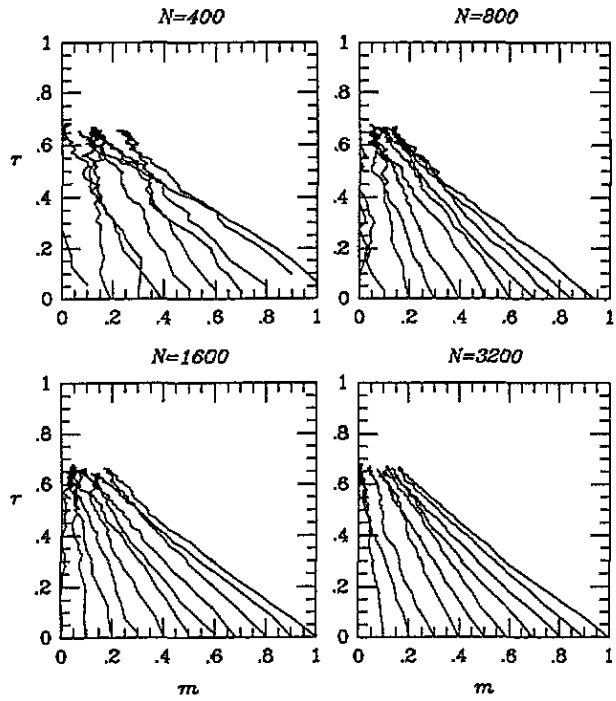

Figure 1. Trajectories in the (m, r) plane obtained by performing sequential simulations of the SK model with $T = 0.1$, $J = 1$ and $J_0 = 0$, for $t \leqslant 10$ iterations/spin.

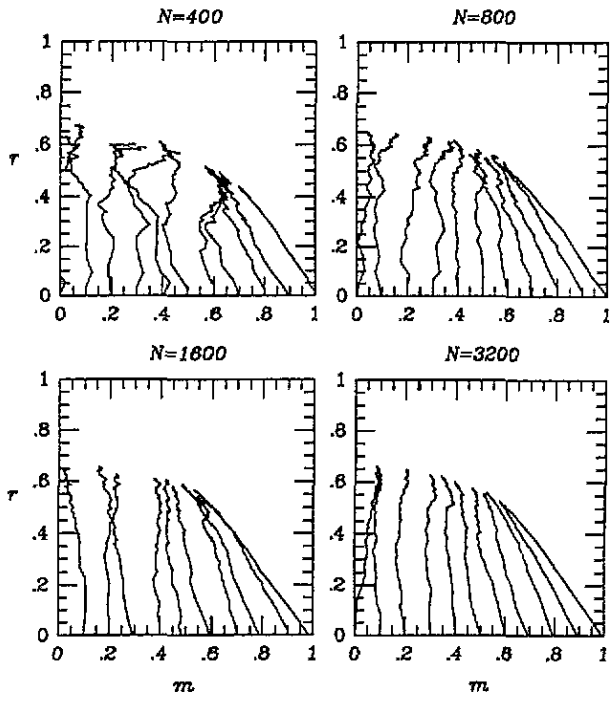

Figure 2. Trajectories in the (m, r) plane obtained by performing sequential simulations of the SK model with $T = 0.1$, $J = 1$ and $J_0 = 1$, for $t \leqslant 10$ iterations/spin.

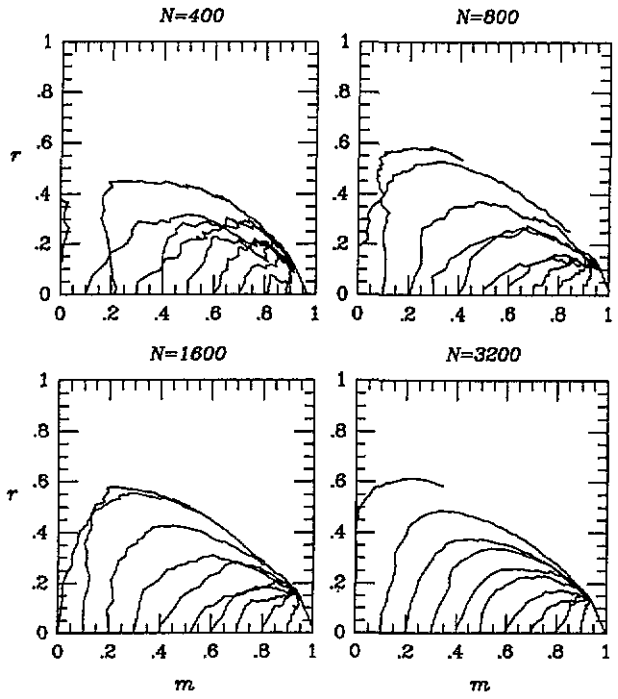

Figure 3. Trajectories in the (m, r) plane obtained by performing sequential simulations of the SK model with $T = 0.1$, $J = 1$ and $J_0 = 2$, for $t \leqslant 10$ iterations/spin.

which allows us to write (11) in the replica form. By writing the delta-functions in integral representation we obtain

$$D_{m,r}[z] = \int \frac{\mathrm{d}x}{2\pi} \mathrm{e}^{\mathrm{i}xz} \lim_{n\to 0} \left[\frac{N}{2\pi}\right]^{2n} \int \mathrm{d}\hat{m}\, \mathrm{d}\hat{r}\, \mathrm{e}^{\mathrm{i}N\sum_\alpha [r\hat{r}_\alpha + m\hat{m}_\alpha]} \left\langle \mathrm{e}^{-\mathrm{i}\sum_\alpha \hat{m}^\alpha \sum_k \sigma_k^\alpha} M\{\sigma^\alpha\} \right\rangle_{\{\sigma^\alpha\}}$$

with

$$M\{\sigma^\alpha\} \equiv \left\langle \mathrm{e}^{-(\mathrm{i}x/\sqrt{N})\sum_{k>l} z_{lk}\sigma_k^l - (\mathrm{i}/\sqrt{N})\sum_\alpha \hat{r}_\alpha \sum_{k>l} z_{kl}\sigma_k^\alpha\sigma_l^\alpha} \right\rangle_{\{z_{ij}\}}.$$

We now perform the average over the quenched variables $\{z_{ij}\}$ in $M\{\sigma^\alpha\}$, with the result

$$M\{\sigma^\alpha\} = \mathrm{e}^{-x^2/2 - (N/4)\sum_{\alpha\beta}\hat{r}_\alpha q_{\alpha\beta}^2(\sigma)\hat{r}_\beta + \frac{1}{4}[\sum_\alpha \hat{r}_\alpha]^2 - x\sum_\alpha \hat{r}_\alpha q_{1\alpha}(\sigma)\sigma_1^\alpha + \mathcal{O}(1/N)}$$

in which we have introduced the familiar order parameters $q_{\alpha\beta}(\sigma) \equiv (1/N)\sum_i \sigma_i^\alpha \sigma_i^\beta$. If we again introduce appropriate delta-functions,

$$1 = \int \mathrm{d}q\, \delta[q - q(\sigma)] = \left[\frac{N}{2\pi}\right]^{n^2} \int \mathrm{d}\hat{q}\, \mathrm{d}q\, \mathrm{e}^{\mathrm{i}N\sum_{\alpha\beta}\hat{q}_{\alpha\beta}[q_{\alpha\beta} - q_{\alpha\beta}(\sigma)]}$$

we can reduce the spin-averages to single-site ones. The result can than be written in terms of an n-replicated Ising spin $(\sigma_1, \ldots, \sigma_n)$:

$$D_{m,r}[z] = \int \frac{\mathrm{d}x}{2\pi} \mathrm{e}^{-x^2/2+\mathrm{i}xz} \lim_{n\to 0} \left[\frac{N}{2\pi}\right]^{n^2+2n} \int \mathrm{d}\hat{m}\, \mathrm{d}\hat{r}\, \mathrm{d}\hat{q}\, \mathrm{d}q\, \mathrm{e}^{\frac{1}{4}[\sum_\alpha \hat{r}_\alpha]^2 + \mathcal{O}(1/N)}$$
$$\times \mathrm{e}^{N\Psi(\hat{m},\hat{r},\hat{q},q)} \frac{\left\langle \mathrm{e}^{-\sum_\alpha \sigma_\alpha [x\hat{r}_\alpha q_{1\alpha} + \mathrm{i}\hat{m}_\alpha] - \mathrm{i}\sum_{\alpha\beta} \hat{q}_{\alpha\beta}\sigma_\alpha\sigma_\beta}\right\rangle_\sigma}{\left\langle \mathrm{e}^{-\mathrm{i}\sum_\alpha \hat{m}_\alpha\sigma_\alpha - \mathrm{i}\sum_{\alpha\beta}\hat{q}_{\alpha\beta}\sigma_\alpha\sigma_\beta}\right\rangle_\sigma} \tag{12}$$

$$\Psi(\hat{m},\hat{r},\hat{q},q) = \mathrm{i}\sum_\alpha [r\hat{r}_\alpha + m\hat{m}_\alpha] + \mathrm{i}\sum_{\alpha\beta} \hat{q}_{\alpha\beta} q_{\alpha\beta} - \tfrac{1}{4}\sum_{\alpha\beta} \hat{r}_\alpha q_{\alpha\beta}^2 \hat{r}_\beta$$
$$+ \log\left\langle \mathrm{e}^{-\mathrm{i}\sum_\alpha \hat{m}_\alpha\sigma_\alpha - \mathrm{i}\sum_{\alpha\beta}\hat{q}_{\alpha\beta}\sigma_\alpha\sigma_\beta}\right\rangle_\sigma .$$

For large N the integral is evaluated by steepest descent and we obtain

$$D_{m,r}[z] = \int \frac{\mathrm{d}x}{2\pi} \mathrm{e}^{-x^2/2+\mathrm{i}xz} \lim_{n\to 0} \frac{\left\langle \mathrm{e}^{-\sum_\alpha \sigma_\alpha [x\hat{r}_\alpha q_{1\alpha} + \mathrm{i}\hat{m}_\alpha] - \mathrm{i}\sum_{\alpha\beta} \hat{q}_{\alpha\beta}\sigma_\alpha\sigma_\beta}\right\rangle_\sigma}{\left\langle \mathrm{e}^{-\mathrm{i}\sum_\alpha \hat{m}_\alpha\sigma_\alpha - \mathrm{i}\sum_{\alpha\beta}\hat{q}_{\alpha\beta}\sigma_\alpha\sigma_\beta}\right\rangle_\sigma} \tag{13}$$

in which the order parameters $\{\hat{m}, \hat{r}, \hat{q}, q\}$ are found by selecting the saddle point of Ψ (12), which gives a minimum with respect to variation of the order parameters $q_{\alpha\beta}$. Variation of $q_{\alpha\beta}$ allows us to already eliminate one set of conjugate parameters: $\hat{q}_{\alpha\beta} = -\frac{1}{2}\mathrm{i} q_{\alpha\beta}\hat{r}_\alpha\hat{r}_\beta$. The remaining conjugate parameters, uniquely determined by the saddle-point requirement, turn out to be purely imaginary: $\hat{r}_\alpha \equiv \mathrm{i}\rho_\alpha$ and $\hat{m}_\alpha \equiv \mathrm{i}\mu_\alpha$, with which we obtain the following *saddle-point equations*:

$$m = \frac{\left\langle \sigma_\alpha \mathrm{e}^{\sum_\gamma \mu_\gamma\sigma_\gamma + \frac{1}{2}\sum_{\gamma\delta} q_{\gamma\delta}\rho_\gamma\rho_\delta\sigma_\gamma\sigma_\delta}\right\rangle_\sigma}{\left\langle \mathrm{e}^{\sum_\gamma \mu_\gamma\sigma_\gamma + \frac{1}{2}\sum_{\gamma\delta} q_{\gamma\delta}\rho_\gamma\rho_\delta\sigma_\gamma\sigma_\delta}\right\rangle_\sigma} \tag{14}$$

$$q_{\alpha\beta} = \frac{\left\langle \sigma_\alpha\sigma_\beta \mathrm{e}^{\sum_\gamma \mu_\gamma\sigma_\gamma + \frac{1}{2}\sum_{\gamma\delta} q_{\gamma\delta}\rho_\gamma\rho_\delta\sigma_\gamma\sigma_\delta}\right\rangle_\sigma}{\left\langle \mathrm{e}^{\sum_\gamma \mu_\gamma\sigma_\gamma + \frac{1}{2}\sum_{\gamma\delta} q_{\gamma\delta}\rho_\gamma\rho_\delta\sigma_\gamma\sigma_\delta}\right\rangle_\sigma} \tag{15}$$

$$\sum_\beta q_{\alpha\beta}^2 \rho_\beta = 2r . \tag{16}$$

The exponent Ψ can be simplified to

$$\Psi = -r\sum_\alpha \rho_\alpha - m\sum_\alpha \mu_\alpha - \tfrac{1}{4}\sum_{\alpha\gamma} \rho_\alpha q_{\alpha\gamma}^2 \rho_\gamma + \log\left\langle \mathrm{e}^{\sum_\gamma \mu_\gamma\sigma_\gamma + \frac{1}{2}\sum_{\gamma\delta} q_{\gamma\delta}\rho_\gamma\rho_\delta\sigma_\gamma\sigma_\delta}\right\rangle_\sigma \tag{17}$$

and the distribution $D_{mr}[z]$ becomes

$$D_{m,r}[z] = \int \frac{\mathrm{d}x}{2\pi} \mathrm{e}^{-x^2/2+\mathrm{i}xz} \lim_{n\to 0} \frac{\left\langle \mathrm{e}^{-\mathrm{i}x\sum_\gamma \sigma_\gamma\rho_\gamma q_{1\gamma} + \sum_\gamma \mu_\gamma\sigma_\gamma + \frac{1}{2}\sum_{\gamma\delta} q_{\gamma\delta}\rho_\gamma\rho_\delta\sigma_\gamma\sigma_\delta}\right\rangle_\sigma}{\left\langle \mathrm{e}^{\sum_\gamma \mu_\gamma\sigma_\gamma + \frac{1}{2}\sum_{\gamma\delta} q_{\gamma\delta}\rho_\gamma\rho_\delta\sigma_\gamma\sigma_\delta}\right\rangle_\sigma} . \tag{18}$$

The physical meaning of the order parameters $q_{\alpha\beta}$, which in the present theory are functions of the two macroscopic state variables m and r, can be inferred in the usual manner by considering two spin systems, σ and σ', with the same microscopic realizations of the quenched disorder. For such systems we define the disorder-averaged probability distribution $P_{mr}(q)$ for the mutual overlap between microscopic configurations if both systems are constrained on the same macroscopic (m, r) subshell:

$$P_{mr}(q) \equiv \left\langle \frac{\sum_{\sigma,\sigma'} \delta\left[q - \frac{1}{N}\sum_k \sigma_k\sigma_k'\right] \delta[m-m(\sigma)]\delta[r-r(\sigma)]\delta[m-m(\sigma')]\delta[r-r(\sigma')]}{\sum_{\sigma,\sigma'} \delta[m-m(\sigma)]\,\delta[r-r(\sigma)]\,\delta[m-m(\sigma')]\,\delta[r-r(\sigma')]} \right\rangle_{\{z_{ij}\}}$$
$$= \lim_{n\to 0} \frac{1}{n(n-1)} \sum_{\alpha\neq\beta} \left\langle \left\langle \delta\left[q - \frac{1}{N}\sum_k \sigma_k^\alpha\sigma_k^\beta\right] \prod_{\gamma=1}^n \delta\left[m-m(\sigma^\gamma)\right]\delta\left[r-r(\sigma^\gamma)\right]\right\rangle_{|\sigma^\gamma|}\right\rangle_{\{z_{ij}\}}$$
$$= \lim_{n\to 0} \frac{1}{n(n-1)} \sum_{\alpha\neq\beta} \delta[q - q_{\alpha\beta}] . \tag{19}$$

This dynamical equivalent of Parisi's [2] equilibrium order-parameter function will, in the present theory, depend on time through the values of the two macroscopic parameters (m, r).

The saddle-point exponent Ψ that is extremized in the replica calculation of the local field distribution has an entropic physical interpretation. We define the entropy per spin $\tilde{S}$ for the instantaneous macroscopic state (m, r) as

$$\tilde{S} \equiv \lim_{N\to\infty} \frac{1}{N} \log \sum_{\sigma} \delta[m - m(\sigma)]\,\delta[r - r(\sigma)] \,. \tag{20}$$

Using the replica trick $\log Z = \lim_{n\to 0}(1/n)[Z^n - 1]$ and averaging over the quenched disorder allows us to express $\tilde{S}$ in terms of the saddle-point problem encountered in calculating $D_{mr}[z]$:

$$\begin{aligned}\tilde{S} &= \log 2 + \lim_{N\to\infty}\lim_{n\to 0} \frac{1}{Nn}\left[\left\langle\left\langle \prod_{\alpha=1}^{n} \delta[m - m(\sigma^\alpha)]\delta[r - r(\sigma^\alpha)]\right\rangle\right\rangle_{\{\sigma^\alpha\},\{z_{ij}\}} - 1\right] \\ &= \log 2 + \lim_{n\to 0} \frac{1}{n}\Psi \end{aligned} \tag{21}$$

in which Ψ is the saddle-point exponent (17). The entropy $\tilde{S}$ again depends on time through the values of the macroscopic state variables (m, r).

2.4. *Equilibrium*

For large times the microscopic probability distribution $p_t(\sigma)$ converges to the static Boltzmann expression $Z^{-1}e^{-\beta H(\sigma)}$ (with the partition function $Z \equiv \sum_\sigma e^{-\beta H(\sigma)}$). Since $H(\sigma)$ (4) can be written in terms of the macroscopic state variables $m(\sigma)$ and $r(\sigma)$, at equilibrium we automatically obtain equipartitioning of probability in the (m, r) sub-shells of the ensemble (equipartitioning in the energy shells is an even stronger statement). This removes the need for the second of our closure assumptions, leaving only the need for our assumption that the evolution of m and r be self-averaging. We will now demonstrate that in equilibrium we do recover the full standard results from equilibrium statistical mechanics, including the replica-symmetry breaking (RSB) equations.

The standard replica formalism as applied to the SK model (see, for example, [3, 4]) leads in the thermodynamic limit $N \to \infty$ to the following expressions for the disorder-averaged free energy per spin $\overline{f}$:

$$\begin{aligned}\overline{f} &= -\frac{1}{\beta}\log 2 + \lim_{n\to 0} \min\ F(m, q) \\ F(m, q) &\equiv \frac{J_0}{2n}\sum_\alpha m_\alpha^2 + \frac{\beta J^2}{4n}\sum_{\alpha\gamma} q_{\alpha\gamma}^2 - \frac{1}{\beta n}\log\left\langle e^{\beta\sum_\alpha \sigma_\alpha(J_0 m_\alpha + \theta) + \frac{1}{2}\beta^2 J^2 \sum_{\alpha\gamma}\sigma_\alpha\sigma_\gamma q_{\alpha\gamma}}\right\rangle_\sigma .\end{aligned} \tag{22}$$

The corresponding saddle-point equations are

$$m_\gamma = \frac{\left\langle \sigma_\gamma e^{\beta\sum_\alpha \sigma_\alpha(J_0 m_\alpha + \theta) + \frac{1}{2}\beta^2 J^2 \sum_{\alpha\gamma}\sigma_\alpha\sigma_\gamma q_{\alpha\gamma}}\right\rangle_\sigma}{\left\langle e^{\beta\sum_\alpha \sigma_\alpha(J_0 m_\alpha + \theta) + \frac{1}{2}\beta^2 J^2 \sum_{\alpha\gamma}\sigma_\alpha\sigma_\gamma q_{\alpha\gamma}}\right\rangle_\sigma} \tag{23}$$

$$q_{\gamma\delta} = \frac{\left\langle \sigma_\gamma\sigma_\delta e^{\beta\sum_\alpha \sigma_\alpha(J_0 m_\alpha + \theta) + \frac{1}{2}\beta^2 J^2 \sum_{\alpha\gamma}\sigma_\alpha\sigma_\gamma q_{\alpha\gamma}}\right\rangle_\sigma}{\left\langle e^{\beta\sum_\alpha \sigma_\alpha(J_0 m_\alpha + \theta) + \frac{1}{2}\beta^2 J^2 \sum_{\alpha\gamma}\sigma_\alpha\sigma_\gamma q_{\alpha\gamma}}\right\rangle_\sigma} \tag{24}$$

and the physical interpretation in terms of the two (disorder-averaged) functions $P(q)$ and $P(m)$ is

$$P(q) \equiv \left\langle Z^{-2}\sum_{\sigma\sigma'}\delta\left[q - \frac{1}{N}\sum_k \sigma_k\sigma_k'\right] e^{-\beta H(\sigma) - \beta H(\sigma')}\right\rangle_{\{z_{ij}\}}$$

$$= \lim_{n\to 0} \frac{1}{n(n-1)} \sum_{\alpha\neq\gamma} \delta[q - q_{\alpha\gamma}] \tag{25}$$

$$P(m) \equiv \left\langle Z^{-1} \sum_{\sigma} \delta\left[m - \frac{1}{N}\sum_{k}\sigma_k\right] e^{-\beta H(\sigma)} \right\rangle_{\{z_{ij}\}}$$

$$= \lim_{n\to 0} \frac{1}{n} \sum_{\alpha} \delta[m - m_\alpha] \,. \tag{26}$$

According to Parisi's [2] theory the magnetization is self-averaging, even in the regime where replica symmetry is broken [20], so $P(m)$ is a delta-function and $m_\alpha = m$ for all α. From the internal energy in thermal equilibrium $E/N = [1 + \beta\partial_\beta]\overline{f}$, which is also self-averaging [20], we obtain the equilibrium expression for our dynamic-order parameter r:

$$r_{eq} = \tfrac{1}{2}\beta J \left[1 - \int dq\, P(q) q^2\right] .$$

For $\beta J_0 < 1$, where $m_{eq} = 0$, the continuous transition at $\beta J = 1$ from the paramagnetic phase with $P(q) = \delta(q)$ to the spin-glass phase, is therefore marked by $r_{eq} = \frac{1}{2}$.

Comparison with the dynamical equations (14)–(16), shows that the two approaches yield identical equations if we impose the following conditions:

$$\mu_\alpha = \mu \equiv \beta(J_0 m + \theta) \qquad \rho_\alpha = \rho \equiv \beta J \,. \tag{27}$$

Below we show that these conditions turn out to be precisely those which imply dynamical stability with respect to the macroscopic flow (8) and (9):

$$\frac{d}{dt} m = 0 \qquad \frac{d}{dt} r = 0$$

and hence they also describe the same equilibrium physics.

First we consider the evolution of m, using the noise distribution (18) and the conditions (27). If we perform a shift of the integration line for z and perform the integral over x we arrive at

$$\frac{d}{dt} m = -m + \lim_{n\to 0} \int Dz \, \frac{\left\langle \tanh[\rho z + \mu + \rho^2 \textstyle\sum_\alpha q_{1\alpha}\sigma_\alpha]\, e^{\mu \sum_\gamma \sigma_\gamma + \frac{1}{2}\rho^2 \sum_{\gamma\delta} q_{\gamma\delta}\sigma_\gamma\sigma_\delta} \right\rangle_\sigma}{\left\langle e^{\mu \sum_\gamma \sigma_\gamma + \frac{1}{2}\rho^2 \sum_{\gamma\delta} q_{\gamma\delta}\sigma_\gamma\sigma_\delta} \right\rangle_\sigma}$$

with the abbreviation $Dz \equiv (2\pi)^{-1/2} e^{-1/2z^2}\, dz$. In the numerator of this expression we perform the average over σ_1 explicitly, and use the identity

$$e^{-u} \int Dz \, \tanh\left[\rho z - \rho^2 + u\right] + e^{u} \int Dz \, \tanh\left[\rho z + \rho^2 + u\right] = 2\sinh[u] \tag{28}$$

to arrive at

$$\frac{d}{dt} m = -m + \lim_{n\to 0} \frac{\left\langle \sigma_1\, e^{\mu \sum_\gamma \sigma_\gamma + \frac{1}{2}\rho^2 \sum_{\gamma\delta} q_{\gamma\delta}\sigma_\gamma\sigma_\delta} \right\rangle_\sigma}{\left\langle e^{\mu \sum_\gamma \sigma_\gamma + \frac{1}{2}\rho^2 \sum_{\gamma\delta} q_{\gamma\delta}\sigma_\gamma\sigma_\delta} \right\rangle_\sigma} = 0$$

(utilizing (14)).

In a similar way we obtain for the evolution of r

$$\frac{d}{dt} r = -2r + \lim_{n\to 0} \int Dz \times \frac{\left\langle \left[z + \rho \textstyle\sum_\alpha q_{1\alpha}\sigma_\alpha\right] \tanh\left[\rho z + \mu + \rho^2 \textstyle\sum_\alpha q_{1\alpha}\sigma_\alpha\right] e^{\mu \sum_\gamma \sigma_\gamma + \frac{1}{2}\rho^2 \sum_{\gamma\delta} q_{\gamma\delta}\sigma_\gamma\sigma_\delta} \right\rangle_\sigma}{\left\langle e^{\mu \sum_\gamma \sigma_\gamma + \frac{1}{2}\rho^2 \sum_{\gamma\delta} q_{\gamma\delta}\sigma_\gamma\sigma_\delta} \right\rangle_\sigma} .$$

Again we perform the average over σ_1 in the numerator explicitly and simplify the result with the identity

$$e^{-u}\int Dz\left[\rho z-\rho^2+u\right]\tanh\left[\rho z-\rho^2+u\right]+e^{u}\int Dz\left[\rho z+\rho^2+u\right]\tanh\left[\rho z+\rho^2+u\right]$$
$$=2u\sinh[u]+2\rho^2\cosh[u] \tag{29}$$

and arrive at

$$\frac{d}{dt}r=-2r+\lim_{n\to 0}\left\{\rho+\rho\sum_{\alpha>1}q_{1\alpha}\frac{\langle\sigma_1\sigma_\alpha\, e^{\mu\sum_\gamma\sigma_\gamma+\frac{1}{2}\rho^2\sum_{\gamma\delta}q_{\gamma\delta}\sigma_\gamma\sigma_\delta}\rangle_\sigma}{\langle e^{\mu\sum_\gamma\sigma_\gamma+\frac{1}{2}\rho^2\sum_{\gamma\delta}q_{\gamma\delta}\sigma_\gamma\sigma_\delta}\rangle_\sigma}\right\}=\lim_{n\to 0}\rho\sum_\alpha q_{1\alpha}^2-2r=0$$

(utilizing (15) and (16)).

Finally we use the equilibrium conditions (27) to show that the thermodynamic entropy per spin $S=\beta^2\partial_\beta\overline{f}$ in equilibrium coincides with the dynamic entropy per spin $\tilde{S}$ given by (20):

$$S=\log 2-\lim_{n\to 0}\left\{m\mu+\frac{3\rho^2}{4n}\sum_{\alpha\gamma}q_{\alpha\gamma}^2-\frac{1}{n}\log\left\langle e^{\mu\sum_\alpha\sigma_\alpha+\frac{1}{2}\rho^2\sum_{\alpha\gamma}\sigma_\alpha\sigma_\gamma q_{\alpha\gamma}}\right\rangle_\sigma\right\}.$$

According to (17) and (21) this expression is identical to the one we obtained for $\tilde{S}$.

3. Replica symmetry

3.1. Replica-symmetric local field distribution

We first make the replica-symmetric ansatz (RS) and assume $P_{mr}(q)$ (19) to be a delta-function, so $q_{\alpha\beta}=\delta_{\alpha\beta}+q(1-\delta_{\alpha\beta})$. From this ansatz the saddle-point equations (14)–(16) allow us to deduce $\mu_\alpha=\mu$ and $\rho_\alpha=\rho$. For $n\to 0$ we obtain

$$m=\int Du\,\tanh(\rho\sqrt{q}u+\mu) \tag{30}$$

$$q=\int Du\,\tanh^2(\rho\sqrt{q}u+\mu) \tag{31}$$

$$\rho=\frac{2r}{1-q^2}. \tag{32}$$

The corresponding local field distribution $D_{mr}^{RS}[z]$ becomes

$$D_{mr}^{RS}[z]=\int\frac{dx}{2\pi}e^{-x^2/2+ixz}\lim_{n\to 0}\int Du\cosh[\rho\sqrt{q}u+\mu-ix\rho]\cosh^{n-1}[\rho\sqrt{q}u+\mu-ixq\rho].$$

We first perform the shift $u\to v+ix\sqrt{q}$, after which the limit $n\to 0$ can be safely taken. In the resulting expression we can perform the integral over x. After some final transformations of integration variables we arrive at

$$D_{mr}^{RS}[z]=\frac{e^{-\frac{1}{2}[z+\rho(1-q)]^2}}{2\sqrt{2\pi}}\left\{1+\int Dy\,\tanh\left[\rho y\sqrt{q(1-q)}-\rho q[z+\rho(1-q)]-\mu\right]\right\}$$
$$+\frac{e^{-\frac{1}{2}[z-\rho(1-q)]^2}}{2\sqrt{2\pi}}\left\{1+\int Dy\,\tanh\left[\rho y\sqrt{q(1-q)}+\rho q[z-\rho(1-q)]+\mu\right]\right\}. \tag{33}$$

This expression cannot be simplified further, except for three special cases which we will discuss below.

From expression (33) and the saddle-point equations it is clear that $D_{mr}^{\mathrm{RS}}[z]$ is Gaussian only along the line $r = 0$:

$$r = 0: \qquad D_{m,0}^{\mathrm{RS}}[z] = \frac{1}{\sqrt{2\pi}} \mathrm{e}^{-z^2/2}. \tag{34}$$

For $r = 0$ we obtain $q = m^2$. We can identify such macroscopic states as purely ferromagnetic (for $m \neq 0$) or paramagnetic (for $m = 0$). The result (34) is indeed what one would obtain in thermal equilibrium for $\beta J = 0$ (where only the paramagnetic and purely ferromagnetic states are found).

A second simplification of (33) results for $q = 0$ (the paramagnetic state), which can only occur along the line $m = 0$. For $m = 0$ the RS saddle-point equations reduce to

$$q = F(q) \equiv \int \mathrm{D}u \, \tanh^2\left[\frac{2ur\sqrt{q}}{1-q^2}\right]$$

with the properties

$$F(1) = 1 \qquad F(q) = 4r^2 q - 32r^4 q^2 + \mathcal{O}(q^3)$$

from which we conclude that along the $m = 0$ line we find a paramagnetic ($q = 0$) state for $r < \frac{1}{2}$:

$$m = 0 \qquad r < \tfrac{1}{2} \qquad D_{0,r}^{\mathrm{RS}}[z] = \frac{1}{2\sqrt{2\pi}} \mathrm{e}^{-\frac{1}{2}[z+2r]^2} + \frac{1}{2\sqrt{2\pi}} \mathrm{e}^{-\frac{1}{2}[z-2r]^2}. \tag{35}$$

This result is indeed what one would obtain for the field distribution in thermal equilibrium in the paramagnetic region of the phase diagram [25]. For $r > \frac{1}{2}$, $m = 0$ we obtain a spin-glass with $q \neq 0$, where again we know from equilibrium studies [25] that the local field distribution indeed has a non-trivial form like that in (33).

The third simplification occurs for $q \approx 1$. Expanding the saddle-point equations in powers of $\epsilon \equiv 1 - q$ gives the leading orders

$$\rho = r\epsilon^{-1} + \cdots \qquad \mu = r\epsilon^{-1}\sqrt{2}\,\mathrm{erf}^{-1}(m) + \cdots \tag{36}$$

$$r = \sqrt{\frac{2}{\pi}} \mathrm{e}^{-[\mathrm{erf}^{-1}(m)]^2}. \tag{37}$$

Equation (37) defines the line in the (m, r) plane where the situation $q = 1$ actually occurs. Near this line we can use the scaling relations (36) to show that (33) reduces to the Schowalter–Klein [26] form, which in equilibrium would be obtained in the limit of zero temperature [25] (in RS approximation):

$$D_{m,r(m)}^{\mathrm{RS}}[z] = \frac{\mathrm{e}^{-\frac{1}{2}[z+r(m)]^2}}{\sqrt{2\pi}} \theta\left[-z - r(m) - \sqrt{2}\,\mathrm{erf}^{-1}(m)\right] + \frac{\mathrm{e}^{-\frac{1}{2}[z-r(m)]^2}}{\sqrt{2\pi}} \theta\left[z - r(m) + \sqrt{2}\,\mathrm{erf}^{-1}(m)\right] \tag{38}$$

in which $r(m)$ denotes the $q = 1$ line (37).

3.2. Special lines in the flow diagram

In order to check the applicability of the RS ansatz we calculate the equivalent of the RS zero-entropy ('freezing') line in the (m, r) plane (where the number of microscopic configurations contributing to our averages vanishes), and the de Almeida–Thouless (AT) line [23], where a replica-symmetry breaking (RSB) solution of the saddle-point equations bifurcates from the RS saddle point.

In RS theory the dynamic entropy (20) is, according to (21), given by

$$\tilde{S}_{\mathrm{RS}} = \log 2 + \int \mathrm{D}u \, \log\cosh[\rho u\sqrt{q} + \mu] - m\mu + \tfrac{1}{4}\rho^2(1-q)^2 - \rho r \,. \tag{39}$$

For $r = 0$ (where there is no spin-glass alignment) the entropy reduces to

$$\tilde{S}_{\mathrm{RS},r=0} = \log 2 - \int_0^{\tanh^{-1}(|m|)} \mathrm{d}s \, s\left[1 - \tanh^2(s)\right] \in [0, \log 2]$$

with $\tilde{S}_{\mathrm{RS},r=0} = \log 2$ at $m = 0$ (the paramagnetic state) down to $\tilde{S}_{\mathrm{RS},r=0} = 0$ at $m = \pm 1$ (the fully ordered ferromagnetic state). Along the line $m = 0$, below $r = \frac{1}{2}$, we find $q = 0$ and $\tilde{S}_{\mathrm{RS}} = \log 2 - r^2 > 0$. Using the scaling relations (36) one can finally show that near the $q = 1$ line (37) the RS entropy is negative, except for $|m| = 1, r = 0$, where the $q = 1$ line and the line $\tilde{S}_{\mathrm{RS}} = 0$ meet. Since the physical dynamical entropy cannot be negative this already signals an inadequacy in the RS ansatz, analogous to that found in the equilibrium RS theory of SK [1]. *The full curve $\tilde{S}_{\mathrm{RS}} = 0$ signals this inadequacy in (m, r) space.*

An AT-line [23] signals the first continuous bifurcation of a saddle-point solution without replica symmetry from the replica-symmetric one. We follow the usual convention and assume that the first such bifurcation is the replicon mode

$$q_{\alpha\beta} \to q + \delta q_{\alpha\beta} \qquad \rho_\alpha = \rho \qquad \mu_\alpha = \mu \,.$$

Inserting this ansatz into the full saddle-point equations shows that the RSB bifurcations are of the form $\sum_{\alpha\neq\beta} \delta q_{\alpha\beta} = 0$. After some bookkeeping and after taking the limit $n \to 0$ one then obtains the bifurcation condition which defines the dynamic AT line

$$1 - \rho^2 \int \mathrm{D}u \, \cosh^{-4}[\rho\sqrt{q}u + \mu] = 0 \,. \tag{40}$$

The RS solution is stable as long as the left-hand side of (40) is positive. For $r = 0$ (with $|m| < 1$) the RS solution is indeed stable. The AT line intersects the line $m = 0$ at $r = \frac{1}{2}$. Using the scaling relations (36) one can also show that near the $q = 1$ line (37) the RS solution is unstable, except for $|m| = 1, r = 0$, where the $q = 1$ line and the AT line meet.

In figure 4 we show the freezing line (where $\tilde{S}_{\mathrm{RS}} = 0$) (39), the AT line (40) and the $q = 1$ line (37) in the (m, r) plane, together with the numerical and analytical flow data. We note that the $q = 1$ line always lies above the $\tilde{S}_{\mathrm{RS}} = 0$ line, which in turn lies above the AT line, except at $|m| = 1, r = 0$. Thus the AT line is the critical one for replica symmetry. The separation between the AT line and the $q = 1$ line, which provides an effective boundary for the (m, r) dynamics, is greatest for small m where the ferromagnetic order is small and occurs for large r, when spin-glass alignment is greatest.

Below the AT line the RS solution is stable against RSB fluctuations. The RS solution breaks down in the region where ferromagnetic order is small and spin-glass-type field-alignment dominates.

3.3. Replica-symmetric flow equations

By combining (8) and (9) with expression (33) we arrive at a closed set of autonomous differential equations describing the deterministic evolution of the macroscopic state (m, r):

$$\frac{\mathrm{d}}{\mathrm{d}t}m = \iint \mathrm{D}x \, \mathrm{D}y \, M(m, r; x, y) - m \tag{41}$$

$$\frac{\mathrm{d}}{\mathrm{d}t}r = \iint \mathrm{D}x \, \mathrm{D}y \, R(m, r; x, y) - 2r \tag{42}$$

in which

$$M(m,r;x,y) = \tfrac{1}{2}\big[1-\tanh\big[x\rho\sqrt{q(1-q)}+\rho q y+\mu\big]\big] \times \tanh\beta[J_0 m+Jy+\theta-J\rho(1-q)] + \tfrac{1}{2}\big[1+\tanh\big[x\rho\sqrt{q(1-q)}+\rho q y+\mu\big]\big]\tanh\beta[J_0 m+Jy+\theta+J\rho(1-q)]$$

$$R(m,r;x,y) = \tfrac{1}{2}[y-\rho(1-q)]\big[1-\tanh\big[x\rho\sqrt{q(1-q)}+\rho q y+\mu\big]\big] \times \tanh\beta[J_0 m+Jy+\theta-J\rho(1-q)] + \tfrac{1}{2}[y+\rho(1-q)]\big[1+\tanh\big[x\rho\sqrt{q(1-q)}+\rho q y+\mu\big]\big] \times \tanh\beta[J_0 m+Jy+\theta+J\rho(1-q)]$$

with $\{q,\rho,\mu\}$ being functions of the macroscopic state (m,r), to be solved from the saddle-point equations (30)–(32).

In figure 4 we compare the flow defined by (41) and (42) with numerical simulations for $N=3000$, $\theta=0$, $J=1$, $J_0\in\{0,1,2\}$ and four choices of the temperature T. The parameters J_0 and T have been chosen in such a way that the corresponding equilibrium situations (according to standard equilibrium theory [4]) include spin-glass states ($J_0<1$, $T<1$), states with ferromagnetic order ($J_0>1$, $T<J_0$) and paramagnetic states ($J_0<T$, $T>1$). At intervals of $\Delta t=1$ iteration/spin we measure the macroscopic-order parameters (m,r) in the simulated system and calculate the derivatives $((\mathrm{d}/\mathrm{d}t)m,(\mathrm{d}/\mathrm{d}t)r)$ as predicted by (41) and (42). The initial states generating the trajectories (labelled by $\ell=0,\ldots,10$) were drawn at random according to $p_0(s)\equiv\prod_i\big[\frac{1}{2}\big[1+\frac{1}{10}\ell\big]\delta_{s_i,\xi_i^1}+\frac{1}{2}\big[1-\frac{1}{10}\ell\big]\delta_{s_i,-\xi_i^1}\big]$, such that that $\langle m\rangle_{t=0}=0.1\ell$ and $\langle r\rangle_{t=0}=1$. The figure indicates that the flow is described quite well by (41) and (42), except for those regions in the (m,r) plane where the RS solution is unstable (above the AT line). More detailed comparisons between theory and simulations will be made in a subsequent section.

From the RS saddle-point equations (30)–(32) we can directly recover all equilibrium results obtained by Sherrington and Kirkpatrick [1,7]. Inserting the two relations $\rho=\beta J$ and $\mu=\beta(J_0 m+\theta)$ into our RS saddle-point equations gives

$$m=\int \mathrm{D}u\ \tanh\beta(J_0 m+J\sqrt{q}u+\theta)$$

$$q=\int \mathrm{D}u\ \tanh^2\beta(J_0 m+J\sqrt{q}u+\theta)$$

$$r=\tfrac{1}{2}\beta J\big[1-q^2\big].$$

We now use the identities (28) and (29) and perform a rotation in the space of the Gaussian integrals in (41) and (42) to arrive for the RS thermal equilibrium state of [1,7] at

$$\frac{\mathrm{d}}{\mathrm{d}t}m=\int \mathrm{D}x\ \tanh\beta(J_0 m+J\sqrt{q}x+\theta)-m=0$$

$$\frac{\mathrm{d}}{\mathrm{d}t}r=\beta J q\left[q-\int \mathrm{D}x\ \tanh^2\beta(J_0 m+J\sqrt{q}x+\theta)\right]=0.$$

The RS order-parameter equations in thermal equilibrium, as derived in [1, 7], thus indeed define fixed-points of our flow equations, as also follows from our more general analysis of section 2.4.

If we insert the fixed-point relations into our expression (40) for the AT line, we obtain

$$1=\beta^2 J^2\int \mathrm{D}x\ \cosh^{-4}\beta(J_0 m+J\sqrt{q}x+\theta)$$

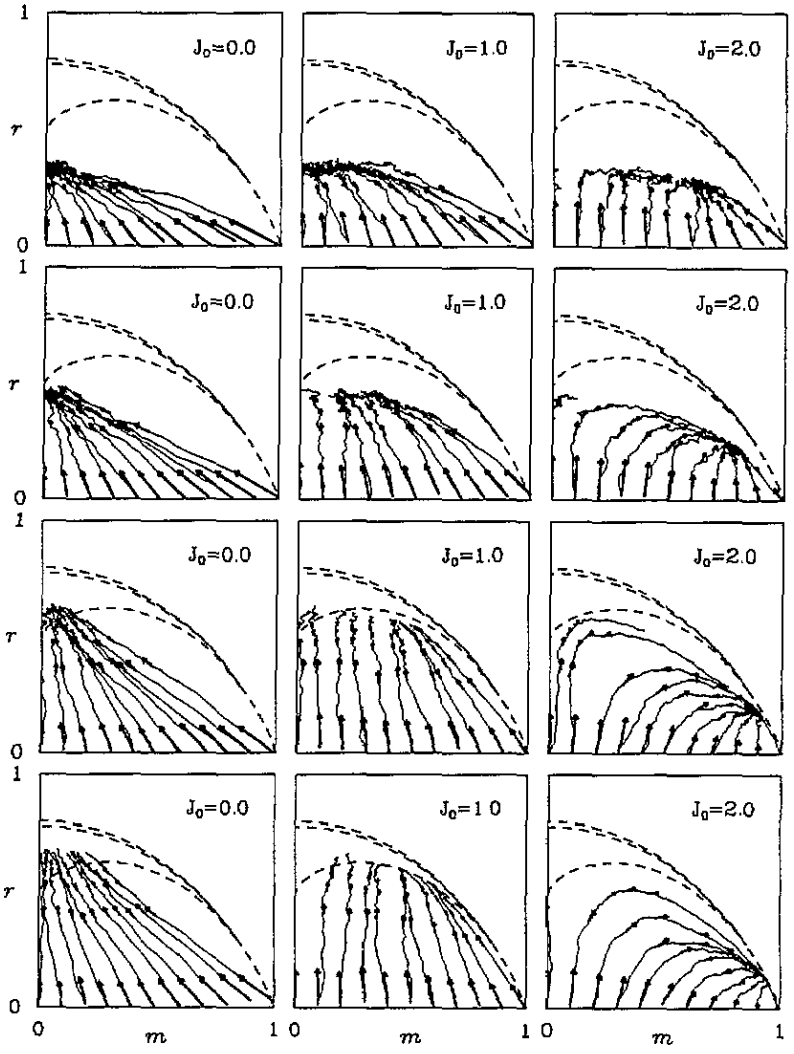

Figure 4. Trajectories in the (m, r) plane obtained by performing sequential simulations of the SK model with $N = 3000$ and zero external field, for $t \leqslant 10$ iterations/spin (full curves), together with the velocities as predicted by the theory (arrows, calculated at intervals of 1 iteration/spin for the instantaneous macroscopic state of the corresponding simulation, at the point of the base of the arrow). The first row of graphs corresponds to $T = 1.5$, the second to $T = 1.0$, the third to $T = 0.5$ and the fourth to $T = 0$. Broken curves indicate the $q = 1$ curve (upper), the RS freezing line (middle) and the AT line (lower).

which, again, corresponds exactly to the result obtained in thermal equilibrium [23]. This includes both the line segment separating paramagnetic from spin-glass phase, where $(m_{\rm eq}, r_{\rm eq}) = \left(0, \frac{1}{2}\right)$, and the line segment separating the replica-symmetric and replica-symmetry broken ferromagnetic phases.

Our dynamical RS laws (41), (42) thus lead precisely to the thermal equilibrium described by Sherrington and Kirkpatrick [1, 7] and de Almeida and Thouless [23], including entropy and stability with respect to replica-symmetry breaking.

4. Further comparisons with numerical simulations

In this section we present some more detailed simulation experiments, the outcome of which is compared to the predictions of our RS theory (the latter need not give sensible results above the AT line). The simulations can display two types of finite-size effects: thermal fluctuations in the flow of the order parameters (i.e. finite-size corrections to the Liouville equation (7)) and fluctuations in the local field distribution (i.e. finite-size corrections to the steepest descent integration leading to (7)).

4.1. The local field distribution

First we compare our analytical result (33) directly with the outcome of measuring the spin-glass contributions to the local alignment fields during actual numerical simulations. In order to probe the different regions of the (m, r) plane we performed simulations from the initial state $(m, r) \sim (0.5, 0)$ for $J_0 = 0$, $J_0 = 1$ and $J_0 = 2$ and measured the instantaneous distribution of the spin-glass contributions to the local alignment fields at different times. In figure 5 we show the resulting trajectories in the (m, r) plane (full curves), together with the AT line (lower broken curve) and the $q = 1$ line (upper broken curve). Dots indicate the instances were the relevant measurements were done: $t = 0$, 1, 5 and 10 (unit: iterations per spin). In figures 6–8 the distributions as measured from the full microstate $\sigma(t)$ (histograms) and calculated from (33) with only $m(t)$ and $r(t)$ as input (broken lines) are shown. The RS theory leading to the distribution (33) turns out to give a good qualitative description of the simulation data; significant deviations are confined to the region above the AT line. Below the AT line these numerical results partially justify *a posteriori* the ansätze of self-averaging and subshell equipartitioning, made to close the set of deterministic dynamical laws for the order parameters m and r.

4.2. Cooling in a small external field

Next we study the evolution in time of the order parameters m and r that results after cooling the system instantaneously from $T = \infty$, the paramagnetic state $(m, r) = (0, 0)$, to $T = 0.1$. For simplicity we choose $J_0 = 0$ and $J = 1$. An external field $\theta = 0.1$ is applied in order to obtain non-trivial evolution for the magnetization (this field being small assures the macroscopic state vector eventually enters into the spin-glass region of the (m, r) flow diagram, above the AT line).

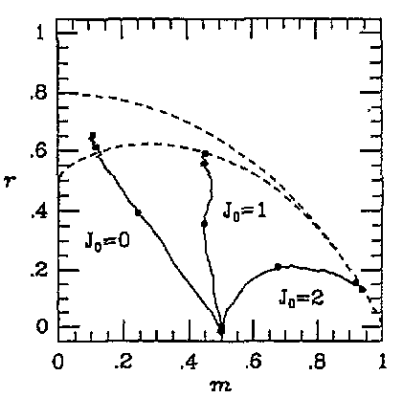

Figure 5. Trajectories in the (m, r) plane obtained from sequential simulations of the SK model with $N = 3200$, $J = 1$ and $T = 0.1$, for three different choices of J_0. Initial states: $(m, r) \sim (0.5, 0)$. Dots indicate times at which the spin-glass contributions to the local fields are measured in order to test the theory.

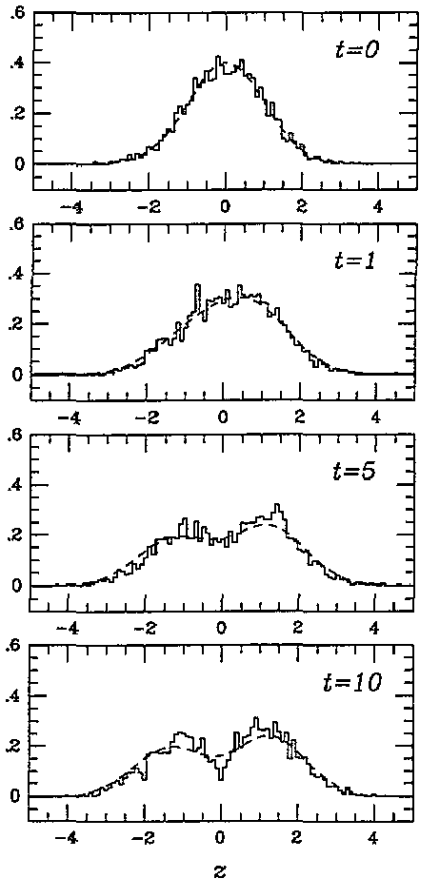

Figure 6. Comparison between RS theory (broken curve) and the local field distribution as measured during the $J_0 = 0$ simulation.

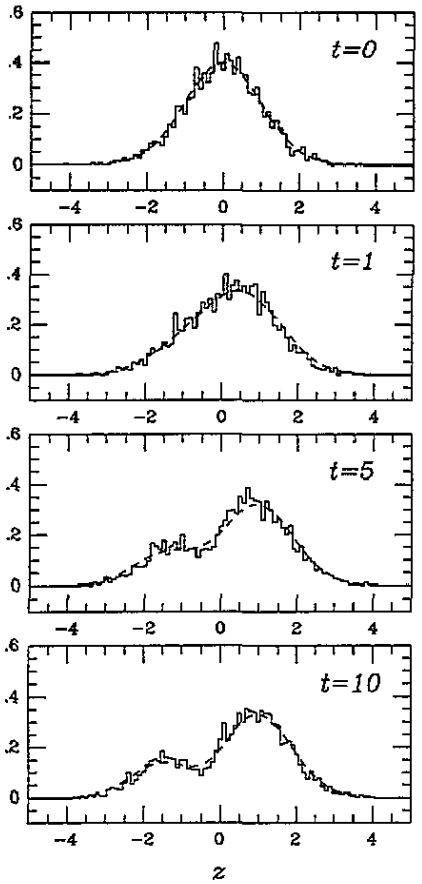

Figure 7. Comparison between RS theory (broken curves) and the local field distribution as measured during the $J_0 = 1$ simulation.

In figures 9 and 10 we compare the result of performing numerical simulations (for an $N = 3200$ system) with the result of solving numerically the RS flow equations (8) and (9). At least within the duration of the numerical experiments ($t \leqslant 10$ iterations/spin), the *direction* of the flow in the (m, r) plane is correctly described by the RS flow equations, even above the AT line. Within the limitations of our simulations the RS theory, however, breaks down even before the AT line is crossed, in that the RS flow equations fail to describe an overall slowing down of the macroscopic flow.

4.3. Decay from a fully magnetized state

Finally we study the relaxation from the fully magnetized initial state $(m, r) = (1, 0)$ (*à la* Kinzel [17], albeit for short time-scales $t \leqslant 10$ only). For simplicity we choose $J_0 = \theta = 0$ and $J = 1$. Figures 11 and 12 show the result of comparing numerical simulations for an $N = 3200$ system with the result of solving numerically the RS flow equations (8) and (9). Again within the duration of the numerical experiments ($t \leqslant 10$ iterations/spin) the *direction* of the flow in the (m, r) plane is correctly described by the RS flow equations, whereas the

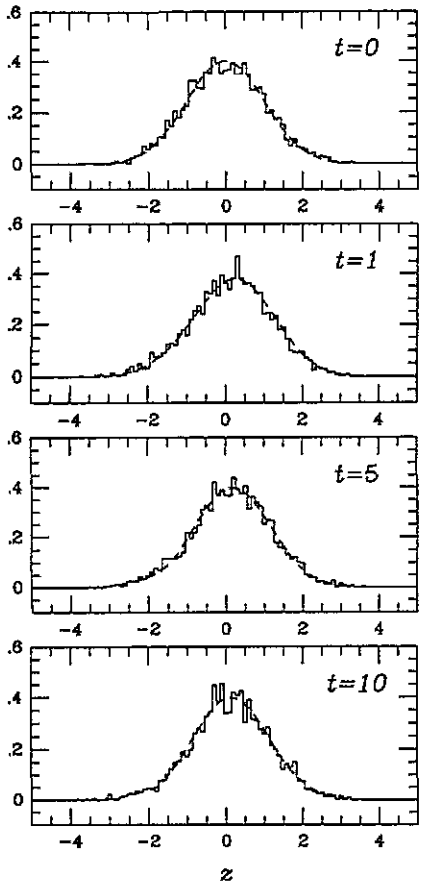

Figure 8. Comparison between RS theory (broken curves) and the local field distribution as measured during the $J_0 = 2$ simulation.

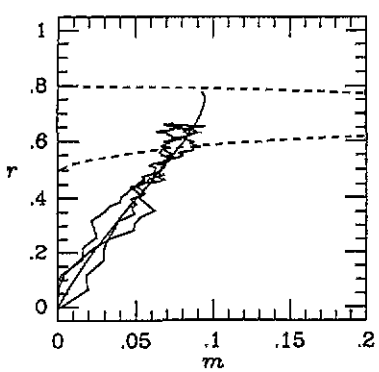

Figure 9. Flow in the (m, r) plane of the order parameters $m(t)$ and $r(t)$, at $T = 0.1$ with a small external field $\theta = 0.1$. Initial state: $(m, r) = (0, 0)$ (the paramagnetic state). Fluctuating curves: three independent $N = 3200$ simulations. Smooth full curve: solution of RS flow equations. Broken curves: the $q = 1$ line (upper) and the AT line (lower).

RS theory apparently fails to describe the overall slowing down that sets in even before the AT line is crossed (which gives rise to the familiar remanent magnetization [17]). In order to describe the slow relaxation of this remanent magnetization above the AT line, measured rather in terms of a few thousand iterations per spin, we clearly need the RSB version of our theory.

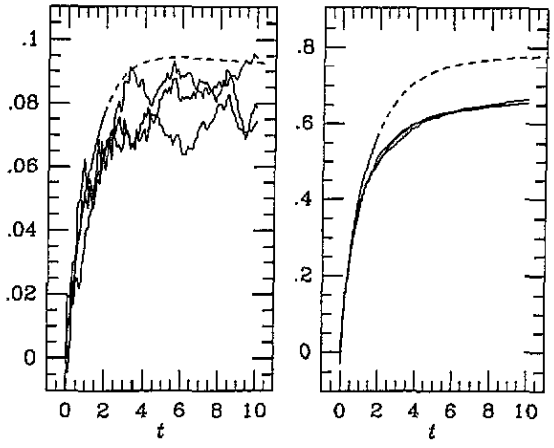

Figure 10. Evolution in time of the order parameters $m(t)$ (left picture) and $r(t)$ (right picture), at $T = 0.1$ with a small external field $\theta = 0.1$. Initial state: $(m, r) = (0, 0)$ (the paramagnetic state). Fluctuating lines: three independent $N = 3200$ simulations. Smooth line: solution of RS flow equations *below* AT line. Broken line: solution of RS flow equations *above* AT line.

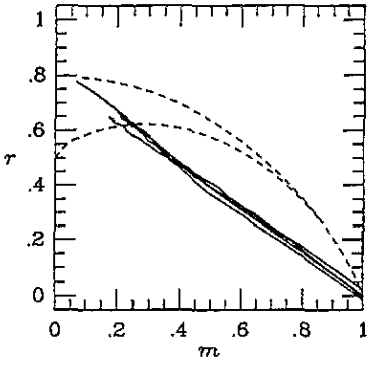

Figure 11. Flow in the (m, r) plane of the order parameters $m(t)$ and $r(t)$, at $T = 0.0$ with $J_0 = \theta = 0$ and $J = 1$ from the fully magnetized initial state $(m, r) = (1, 0)$. Fluctuating curves: three independent $N = 3200$ simulations. Thick full curve: solution of RS flow equations. Broken curve: the $q = 1$ line (upper) and the AT line (lower).

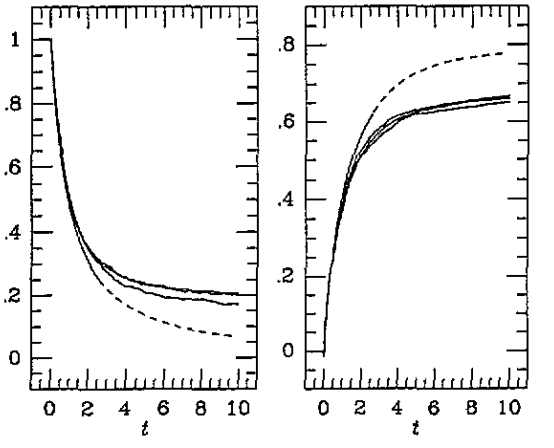

Figure 12. Evolution in time of the order parameters $m(t)$ (left picture) and $r(t)$ (right picture), at $T = 0.0$ with $J_0 = \theta = 0$ and $J = 1$. Fluctuating curves: three independent $N = 3200$ simulations. Smooth curve: solution *of RS flow equations below the AT line*. Broken curve: solution of RS flow equations *above* the AT line.

5. Discussion

In this paper we have developed a dynamical theory, valid on finite time-scales, to describe the Glauber dynamics of the SK model in terms of deterministic flow equations for two macroscopic state variables: the magnetization and the spin-glass contribution to the energy. Two transparant physical assumptions, based on a systematic removal of microscopic

memory effects, allow us to calculate the time-dependent distribution of local aligment fields in terms of the instantaneous order parameters only and thereby obtain a *closed* set of flow equations for our two order parameters. The theory produces, in a natural way, dynamical generalizations of the AT- and zero-entropy lines and of Parisi's order-parameter function $P(q)$. In equilibrium we recover the standard results from equilibrium statistical mechanics, including the full RSB equations.

In calculating the order-parameter flow explicitly we have made the replica-symmetric (RS) ansatz, as a natural first step. A subsequent paper will be devoted to the implications of breaking the replica symmetry (RSB). We found that in most of the flow diagram replica symmetry is stable. Numerical simulations suggest that our equations describe the shape of the local field distribution and the macroscopic dynamics quite well in the region where replica symmetry is stable. In the region of the flow diagram where the RS solution is unstable the flow *direction* as given by the RS theory still seems correct and analysis of the flow equations shows that the RS theory even predicts non-exponential relaxation in the limit $T \to 0$. However, the RS theory fails to describe a rigorous slowing down which, according to simulations, sets in near the de Almeida–Thouless [23] line. Intuitively one expects the breaking up of phase space, as indicated by the breaking of replica symmetry, to have a slowing down effect on the macroscopic flow. Preliminary investigations of the effect of replica-symmetry breaking, based on expansions just above the AT line and on a one-step symmetry breaking *à la* Parisi, show that this is indeed the case [27].

We consider the main appeal of our formalism to be its transparency. The theory is formulated in terms of two directly observable macroscopic state variables: the magnetization and the spin-glass contribution to the energy per spin. Furthermore the macroscopic laws are derived directly from the underlying microscopic stochastic equations, given two key assumptions. An interesting difference with existing (mostly Langevin) approaches is that in the present formalism replica theory enters naturally as a mathematical tool in calculating the time-dependent distribution of local alignment fields. One of the two assumptions on which our analysis is based (self-averaging of the macroscopic laws with respect to the frozen disorder) is quite standard. Both assumptions are supported by evidence from numerical simulations. Based on the agreement between theory and simulations in the RS region we believe that our two closure assumptions lead to a theory which captures the main physics of the order-parameter flow of the SK model on finite time-scales, and that the impact of microscopic memory effects (which in the theory are explicitely removed) can be viewed, as in [21,22], principally as an overall slowing down. Our next step will be to investigate in detail the RSB version of our dynamical laws, which will be the subject of a subsequent paper.

Acknowledgments

We would like to thank L Cugliandolo and J Kurchan for communicating some of their work prior to publication and S Franz for interesting discussions on SK dynamics.

References

[1] Sherrington D and Kirkpatrick S 1975 *Phys. Rev. Lett.* 35 1792
[2] Parisi G 1980 *J. Phys. A: Math. Gen.* 13 1101; 1983 *Phys. Rev. Lett.* 50 1946
[3] Mezard M, Parisis G and Virasoro M A 1987 *Spin Glass Theory and Beyond* (Singapore: World Scientific)
[4] Fisher K H and Hertz J A 1991 *Spin Glasses* (Cambridge: Cambridge University Press)
[5] Edwards S F and Anderson P W 1976 *J. Phys. F: Met. Phys.* 6 1927

[6] Kinzel W and Fisher K H 1977 *Solid State Commun.* **23** 687
[7] Kirkpatrick S and Sherrington D 1978 *Phys. Rev.* B **17** 4384
[8] Sompolinsky H 1981 *Phys. Rev. Lett.* **47** 935
[9] Sompolinsky H and Zippelius A 1982 *Phys. Rev.* B **25** 6860
[10] Horner H 1984 *Z. Phys.* B **57** 29, 39; 1987 *Z. Phys.* B **66** 175
[11] Cugliandolo L F and Kurchan J 1994 *J. Phys. A: Math. Gen.* **27** 5749
[12] Zinn-Justin J 1993 *Quantum Field Theory and Critical Phenomena* (Oxford: Oxford University Press)
[13] Glauber R J 1963 *J. Math. Phys.* **4** 294
[14] Sommers H J 1987 *Phys. Rev. Lett.* **58** 1268
[15] Rieger H, Schreckenberg M and Zittartz J 1989 *Z. Phys.* B **74** 527
[16] Lusakowski A 1991 *Phys. Rev. Lett.* **66** 2543
[17] Kinzel W 1986 *Phys. Rev.* B **33** 5086
[18] Cugliandolo L F, Kurchan J and Ritort F 1994 *Phys. Rev.* B **49** 6331
[19] Vincent E, Hammann J and Ocio M 1992 *Recent Progress in Random Magnets* ed D H Ryan (Singapore: World Scientific)
[20] Mézard M and Virasoro M A 1985 *J. Physique* **46** 1293
[21] Coolen A C C and Sherrington D 1993 *Phys. Rev. Lett.* **71** 3886; 1994 *Phys. Rev.* E **49** 1921
[22] Coolen A C C and Franz S 1994 *J. Phys. A: Math. Gen.* at press
[23] de Almeida J R L and Thouless D J 1978 *J. Phys. A: Math. Gen.* **11** 983
[24] Bedeaux D, Lakatos-Lindenberg K and Shuler K 1971 *J. Math. Phys.* **12** 2116
[25] Thomsen M, Thorpe M F, Choy T C, Sherrington D and Sommers H J 1986 *Phys. Rev.* B **33** 1931
[26] Schowalter L J and Klein M W 1979 *J. Phys. C: Solid State Phys.* **12** L935
[27] Coolen A C C and Sherrington D 1994 in preparation